Estimation of Sea Surface Temperature From Remote Sensing in the 11- to 13-μm Window Region

C. PRABHAKARA

NASA Goddard Space Flight Center, Greenbelt, Maryland 20771

G. DALU

C.N.R. Istituto di Fisica dell'Atmosfera, Rome, Italy

V. G. KUNDE

NASA Goddard Space Flight Center, Greenbelt, Maryland 20771

The Nimbus 3 and 4 Iris spectral data in the 11- to 13-μm water vapor window region are analyzed to determine the sea surface temperature (SST). The high spectral resolution data of Iris are averaged over approximately 1-μm-wide intervals to simulate channels of a radiometer to measure the SST. In the present exploratory study, three such channels in the 775- to 960-cm^{-1} (12.9–10.5 μm) region are utilized to measure the SST over cloud-free oceans. However, two of these channels are sufficient in routine SST determination. The differential absorption properties of water vapor in the two channels enable one to determine the water vapor absorption correction without detailed knowledge of the vertical profiles of temperature and water vapor. The feasibility of determining the SST is demonstrated globally with Nimbus 3 data, where cloud-free areas can be selected with the help of albedo data from the medium-resolution infrared radiometer experiment on board the same satellite. The SST derived from this technique agrees with the measurements made by ships to about 1°C.

One of the techniques used to measure the sea surface temperature (SST) from satellites involves observations of the brightness temperature in the 8- to 13-μm water vapor window region under cloud-free sky conditions. *Allison and Kennedy* [1967], *Smith et al.* [1970], *Shenk and Salomonson* [1972], *Rao et al.* [1972], and others have estimated the SST from remote-sensing window measurements. The principal advantage of this infrared window is that it can be used both night and day. A second advantage is that low noise equivalent temperature may be attained in radiometric measurements, since the terrestrial emission has its peak value in this spectral region.

Several of the earlier attempts to estimate the SST from the window measurements have dealt elaborately with the problem of eliminating cloud contaminated data. The present study does not offer any improvement in this respect. The problem of correcting the window data for water vapor absorption, however, is better resolved in this study.

The brightness temperature in the window, measured from space over a cloud-free ocean, is in general lower than the SST. The water vapor absorption is mainly responsible for this effect. In the earlier studies the water vapor attenuation correction was derived from climatological data on water vapor and temperature in the atmosphere. Such climatological corrections can introduce errors as large as ±2°C into the estimated SST. It is necessary therefore to apply the water vapor correction corresponding to the local vertical distribution of temperature and water vapor to improve the accuracy of the estimated SST. Such soundings from a remote platform would require elaborate instrumentation and data reduction procedures.

Anding and Kauth [1970] and *Price* [1973] have examined the usefulness of differential absorption in the window region to correct for the water vapor absorption with soundings of temperature and water vapor. In this study a transmittance model for the water vapor window region is developed that can be used in a simple scheme that does not require temperature and humidity soundings of the atmosphere to estimate SST over cloud-free oceans with the help of Nimbus 3 and 4 Iris measurements. This scheme takes advantage of the differential absorption properties of the water vapor in the spectral region 775–960 cm^{-1}. With this technique the SST is estimated with an accuracy of about 1°C from Iris measurements.

Transmission of Water Vapor in the 11- to 13-μm Region

It is necessary to model the water vapor absorption in the three spectral regions 775–831, 831–887, and 887–960 cm^{-1}, which are used to simulate the broad-band radiometer channels for the retrieval of the SST. The 1000- to 1100-cm^{-1} region has been avoided owing to the strong ozone absorption. The effects of aerosols are not explicitly considered in this investigation. However, the aerosol effect in the 11- to 13-μm region is expected to be less than 1°C [*Stowe*, 1971].

The total water vapor transmission in the 11-μm window region may be expressed as

$$\tau(\nu, T) = \tau_e(\nu, T)\tau_p(\nu, T)\tau_l(\nu, T) \quad (1)$$

where τ_e and τ_p are associated with the water vapor continuum and τ_l with the water vapor lines.

The laboratory measurements of *Bignell* [1970] and *Burch* [1970] show that the water vapor absorption in the 8- to 13-μm window region is primarily dependent on the water vapor partial pressure e. This absorption is referred to as 'e-type' absorption, one of its characteristics being a strong negative temperature dependence. Water dimer molecules may be responsible for this behavior. Window radiance measurements made by *Platt* [1972] with a radiometer on board an aircraft looking down at the sea surface and measurements made by

Lee [1973] with a balloon-borne radiometer are consistent with the presence of the *e*-type absorption in the atmosphere. Nimbus 4 Iris data reported by *Kunde et al.* [1974] also confirm this type of absorption. *Grassl* [1973] derived the magnitude of the aerosol and *e*-type absorption coefficients in the window region with the help of a ground-based radiometer that measured the sky emission. The absorption coefficients deduced by Grassl are in close agreement with the laboratory data obtained by Bignell and Burch. Grassl also found that in temperate and cold climates the aerosol absorption can be comparable to the *e*-type absorption. *Wark* [1972], *Houghton and Lee* [1972], and *Prabhakara et al.* [1972] have emphasized the importance of *e*-type absorption in determining the SST.

The *e*-type absorption coefficients in the three channels considered here are obtained from the measurements of *Burch* [1970] made at a temperature of 296°K. These absorption coefficients are assumed to decrease at a rate of 2%/1°C [*Bignell*, 1970]. That is,

$$k_e(\nu, T) = k_e(\nu, 296)[1 - 0.02(T - 296)] \quad (2)$$

where

k_e *e*-type absorption coefficient, g^{-1} cm^2;
ν wave number, cm^{-1};
T temperature, degrees Kelvin.

The transmission τ_e is then calculated with the formula

$$\tau_e(\nu, T) = \exp[-k_e(\nu, T)ew] \quad (3)$$

where

e water vapor pressure, atmospheres;
w path length of water vapor, grams per square centimeter.

The water vapor pressure in the atmosphere is assumed to decrease exponentially with height with a constant scale height. This assumption implies that the mean vapor pressure e in a column of the atmosphere is proportional to the total precipitable amount of water w in that column. That is,

$$e = sw \quad (4)$$

where s is a constant.

As a working hypothesis it is assumed that a mean vapor pressure of 3 mbar in an atmospheric column of 1 cm^2 corresponds to 1 g of precipitable water in that column, which means that $s = 3$ mbar g^{-1}.

With these numerical values and with the help of (2) and (3) we have calculated the transmission τ_e for different path lengths at two temperatures, 280° and 300°K.

The second component of the continuum absorption depends on the total pressure:

$$\tau_p(\nu, T) = \exp[-k_p(\nu, T)wp/p_0] \quad (5)$$

where

k_p absorption coefficient for the collision broadening in the wings of water vapor lines, g^{-1} cm^2;
p average pressure of the layer of the atmosphere, weighted according to the distribution of water vapor, assumed to be 850 mbar;
p_0 standard pressure of 1000 mbar.

Only upper limits have been inferred from the laboratory data for the value of k_p. In this study we have adopted the values of k_p used by *Kunde and Maguire* [1974]. This component is only important for low water vapor concentrations ($w < 1$ g cm^{-2}). The absorption model for the water vapor continuum is thus empirical in nature, based entirely on laboratory absorption measurements.

For the spectral lines, *Goody* [1964] has listed the line data of *Benedict and Kaplan* [1959] arranged in 20-cm^{-1} intervals at three temperatures: 220°, 260°, and 300°K. These data are used to calculate the average transmission τ_l due to spectral lines. A statistical band model with nonoverlapping lines, having an exponential line intensity distribution, has been assumed:

$$\tau_l(\nu, T) = 1 - k_l w\left[1 + \frac{k_l w}{(4\alpha_0/\delta)p/p_0}\right]^{-1/2} \quad (6)$$

where

k_l mean absorption coefficient, equal to S/δ, g^{-1} cm^2;
S mean line intensity, g^{-1} cm;
δ average line spacing, cm^{-1};
α_0 line half width at STP, cm^{-1};
p 850 mbar;
p_0 1000 mbar.

The absorption coefficients used are listed in Table 1 for two temperatures, 280° and 300°K. The various transmission values derived in the three spectral intervals at the two different temperatures are shown in Table 2. The total transmission at the two temperatures is plotted in Figure 1 as a function of path length for the three spectral channels. From Figure 1 it is seen that the transmission function to a first approximation is linearly related to the path length up to about 4 g of precipitable water at both temperatures. This approximate linearity of the transmission is also obtained when we assume that the line intensity distribution has the form proposed by *Godson* [1954]. As these temperatures and path lengths cover a wide variety of atmospheric conditions from tropics to high latitudes, it may be stated that this approximate linear law is applicable over most of the globe. By means of the linear property of the transmission function shown in Figure 1 the following equation is developed:

$$\tau(\nu, w, T) \cong 1 - K(\nu)w[1 - \epsilon(T - 296)] \quad (7)$$

where $K(\nu)$ is an effective absorption coefficient corresponding to the total water vapor absorption and the coefficient ϵ accounts for the temperature dependence of $K(\nu)$.

TABLE 1. Water Vapor Absorption Coefficients

Channel	$\Delta\nu$, cm^{-1}	k_p, g^{-1} cm^2		k_e, g^{-1} cm^2		k_l, g^{-1} cm^2		α_0/δ at STP
		280°K	300°K	280°K	300°K	280°K	300°K	
1	775 to 831	0.035	0.040	19.46	13.56	0.333	0.497	0.015
2	831 to 887	0.017	0.020	14.52	10.12	0.098	0.157	0.018
3	887 to 960	0.009	0.010	11.59	8.08	0.047	0.074	0.014

TABLE 2. Water Vapor Transmissivities for 280° and 300°K

	Δν	Precipitable Water, g cm^{-2} 0.5	1	2	3	4	6	8
		Transmissivities for 280°K						
Channel τ_p								
1	775 to 831	0.985	0.970	0.942	0.914	0.887	0.835	0.787
2	831 to 887	0.993	0.986	0.971	0.957	0.944	0.917	0.890
3	887 to 960	0.996	0.992	0.985	0.977	0.970	0.955	0.940
Channel τ_e								
1	775 to 831	0.985	0.943	0.792	0.591	0.393	0.122	0.024
2	831 to 887	0.989	0.957	0.840	0.676	0.498	0.208	0.062
3	887 to 960	0.991	0.966	0.870	0.731	0.573	0.286	0.108
Channel τ_l								
1	775 to 831	0.920	0.880	0.825	0.783	0.748	0.690	0.641
2	831 to 887	0.963	0.939	0.905	0.878	0.856	0.820	0.790
3	887 to 960	0.981	0.967	0.947	0.931	0.917	0.895	0.877
Channel τ								
1	775 to 831	0.893	0.805	0.615	0.423	0.261	0.070	0.012
2	831 to 887	0.946	0.886	0.738	0.568	0.402	0.156	0.044
3	887 to 960	0.968	0.927	0.812	0.665	0.510	0.244	0.089
		Transmissivities for 300°K						
Channel τ_p								
1	775 to 831	0.983	0.967	0.934	0.903	0.873	0.815	0.762
2	831 to 887	0.992	0.983	0.967	0.950	0.934	0.903	0.873
3	887 to 960	0.996	0.992	0.983	0.975	0.967	0.950	0.934
Channel τ_e								
1	775 to 831	0.990	0.960	0.850	0.693	0.521	0.231	0.074
2	831 to 887	0.992	0.970	0.886	0.761	0.615	0.335	0.143
3	887 to 960	0.994	0.976	0.908	0.804	0.678	0.418	0.212
Channel τ_l								
1	775 to 831	0.899	0.851	0.784	0.733	0.691	0.620	0.560
2	831 to 887	0.948	0.917	0.874	0.841	0.814	0.769	0.731
3	887 to 960	0.972	0.954	0.928	0.909	0.892	0.865	0.842
Channel τ								
1	775 to 831	0.875	0.790	0.622	0.459	0.314	0.117	0.032
2	831 to 887	0.933	0.874	0.749	0.608	0.468	0.233	0.091
3	887 to 960	0.962	0.924	0.828	0.713	0.585	0.343	0.167

The transmission functions derived here are dependent on the assumed water vapor distribution in the atmosphere, on the statistical band model, and on the absorption coefficients k_l and k_p. For this reason the magnitude of $K(\nu)$ can change with the choice of the model and the parameters used in the calculations. However, it is found that for a realistic combination of parameters the transmission function $\tau(\nu)$ varies in a nearly linear fashion with respect to path length w. This property is exploited in the present study.

THEORY

In a cloud-free nonscattering atmosphere under local thermodynamic equilibrium the radiative transfer equation for the upwelling intensity $I(\nu)$ may be written as

$$I(\nu) = B(\nu, T_s)\tau(\nu, p_0) + \int_{\tau(\nu,p_0)}^{1} B[\nu, T(p)]\, d\tau(\nu, p) \quad (8)$$

where

- p_0 surface pressure, millibars;
- p pressure at any height, millibars;
- ν wave number, cm^{-1};
- T temperature, degrees Kelvin;
- T_s surface temperature, degrees Kelvin;
- B Planck intensity, ergs cm^{-1} sr^{-1} s^{-1};
- τ transmission from any pressure level p to the top of the atmosphere.

The surface emissivity in (8) is assumed to be unity.

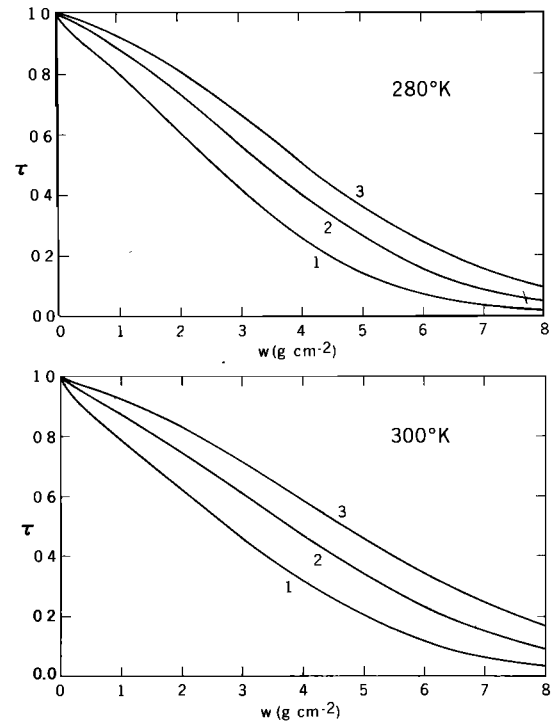

Fig. 1. Water vapor transmission in the three channels as a function of precipitable water content in the atmosphere for T = 280°K and T = 300°K: 1, 775–831 cm^{-1}; 2, 831–887 cm^{-1}; and 3, 887–960 cm^{-1}.

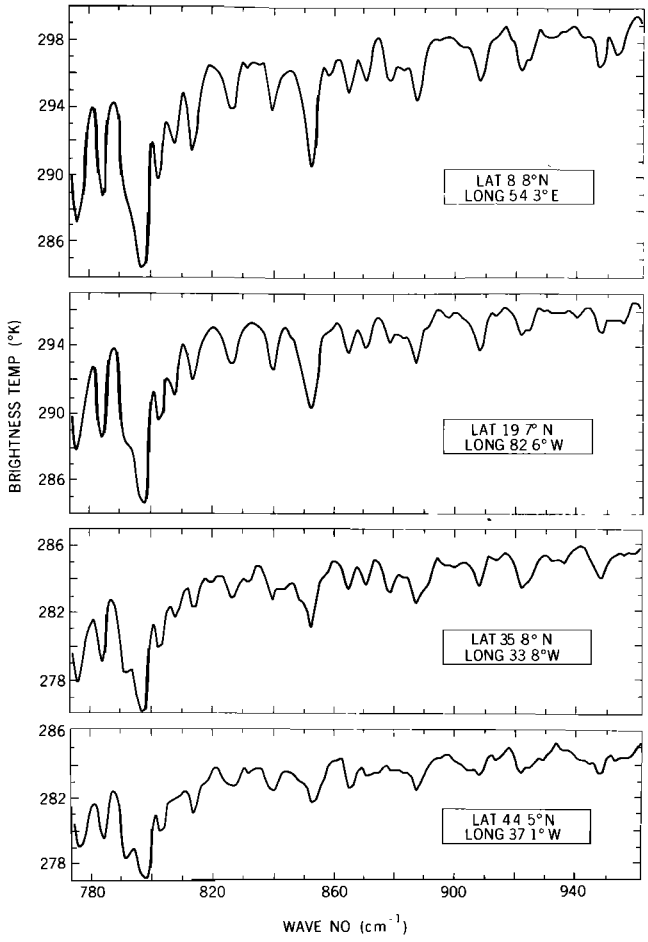

Fig. 2. Cloud-free Nimbus 4 Iris brightness temperature spectra.

Equation (8) may be simplified as

$$I(\nu) = B(\nu, T_s)\tau(\nu, p_0) + \bar{B}(\nu)[1 - \tau(\nu, p_0)] \quad (9)$$

where $\bar{B}(\nu)$ is the weighted mean Planck emission of the atmosphere:

$$\bar{B}(\nu) = \int_{\tau(\nu,p_0)}^{1} B[\nu, T(p)]\, d\tau \Big/ \int_{\tau(\nu,p_0)}^{1} d\tau \quad (10)$$

Substituting (7) into (9), we get

$$I(\nu) \cong B(\nu, T_s) - AK(\nu)[B(\nu, T_s) - \bar{B}(\nu)] \quad (11)$$

where $A = w\{1 - \epsilon[T(p) - 296]\}$ is a constant for a given atmosphere, independent of wave number.

The Planck function B can be expanded about the surface temperature T_s when only the linear terms are retained to yield

$$B(\nu, T) \cong B(\nu, T_s) + \frac{\partial B(\nu, T_s)}{\partial T}(T - T_s) \quad (12)$$

This approximation holds good over a small range of temperatures and a narrow wave number span. With this approximation, (11) becomes

$$T(\nu) \cong T_s - AK(\nu)[T_s - \bar{T}(\nu)] \quad (13)$$

where $T(\nu)$ is the brightness temperature and $\bar{T}(\nu)$ is the equivalent radiative temperature of the atmosphere.

Equation (13) indicates a linear relationship between the observed brightness temperature and the absorption coefficient $K(\nu)$, provided that $\bar{T}(\nu)$ is not strongly dependent on ν. With the help of the radiative transfer equation (8), model calculations based on typical atmospheric temperature and humidity profiles were made to examine the amount by which $\bar{T}(\nu)$ changes with ν. It is found from these model calculations that within the 775- to 960-cm^{-1} region, $\bar{T}(\nu)$ changes with ν by less than 1°C. The magnitude of $[T_s - \bar{T}(\nu)]$ is found to be about 10°C. In view of this, the change in $\bar{T}(\nu)$ is neglected in (13) to arrive at an approximate linear relationship between $T(\nu)$ and $K(\nu)$ as follows:

$$T(\nu) \cong T_s - \beta K(\nu) \quad (14)$$

where $\beta = A[T_s - \bar{T}(\nu)]$ is a constant for a given atmosphere.

Now if we know the brightness temperature $T(\nu)$ in at least two spectral regions, which have appreciable difference in $K(\nu)$, (14) can be used to estimate the sea surface temperature T_s. This formulation does not require explicitly either the temperature and humidity distribution in the atmosphere or the temperature and pressure dependence of the absorption coefficients.

Results and Discussion

The Nimbus 4 Iris had a ~95-km field of view, a 2.8-cm^{-1} spectral resolution, and a noise equivalent radiance of about 0.5 erg cm^{-1} sr^{-1} s^{-1} [*Hanel et al.*, 1972]. These high spectral resolution data reveal the influence of numerous water vapor absorption lines, which are strong in the tropics and decrease in strength at high latitudes. In addition, these spectra indicate that the brightness temperature increases steadily from about 775 to 960 cm^{-1}. This is illustrated in Figure 2, where a few spectra selected over cloud-free oceans are shown. The cloud-free condition is inferred from the Nimbus 4 image dissector camera system pictures [*Sabatini*, 1970]. This procedure is somewhat subjective and is not practical for collecting a large sample of cloud-free spectra. A small sample of eight clear-sky spectra was selected where the SST was available from ship measurements. The mean brightness temperature corresponding to each one of the spectral channels 775–831, 831–887, and 887–960 cm^{-1} is listed in Table 3. From this sample of Iris data and the corresponding observed SST, one can determine the relative values of the three absorption coefficients $K(\nu)$ from (14) for each of the three spectral intervals. A first guess for these coefficients is derived from the synthetic transmission

TABLE 3. Nimbus 4 Iris Window Brightness Temperature and the SST From Iris and Ships

Spectrum	Lat.	Long.	T_1	T_2	T_3	T_{Iris}	T_{ship}
1	41.0°N	62.5°W	272.9	275.2	276.8	281.2	281.0
2	36.6°N	60.9°W	284.5	286.9	287.9	292.0	290.5
3	11.0°N	53.5°W	287.8	291.7	293.4	300.1	300.5
4	35.6°N	33.8°W	281.2	283.8	285.0	289.6	291.0
5	44.6°N	37.1°W	280.9	283.1	284.0	287.7	287.0
6	19.7°N	82.6°W	291.2	294.2	295.6	300.7	301.5
7	15.1°N	144.7°W	292.7	294.9	296.1	300.1	301.2
8	39.4°N	69.1°W	286.9	290.6	291.8	298.0	296.2

TABLE 4. Relative Absorption Coefficient (g^{-1} cm^2) for the Three Window Channels

	Channel 1	Channel 2	Channel 3
$\Delta\nu$	775 to 831	831 to 887	887 to 960
$K(\nu)$	0.191	0.131	0.104

function illustrated in Figure 1*a*, and these values are then adjusted to give a best fit to the data of Table 3. These values of $K(\nu)$ are listed in Table 4. In Figure 3 a plot of the measured brightness temperatures versus $K(\nu)$ for the eight cases is presented to show the degree of linearity in the observed data.

The advantage of using the method presented here to determine the SST is that it is inherently capable of taking into account the effects of water vapor and temperature profiles satisfactorily. This capability is particularly necessary in measuring the SST with meaningful accuracy over the tropics, where the water vapor absorption correction is large and quite variable in time and space. To demonstrate this point, a set of six cloud-free Nimbus Iris spectra from one orbit from 8° to 14°N along 55°E longitude on May 10, 1970, over the Arabian Sea are analyzed. The window brightness temperature in the three channels for each of these six spectra is plotted in Figure 4 as a function of the absorption coefficient $K(\nu)$. The intercept on the ordinate gives the value of the SST. It may be noticed that the Iris window brightness temperature in the most transparent channel (887–960 cm^{-1}) increases by about 3°K northward from 8° to 14°N. One would erroneously infer from a water vapor correction based on climatological atmospheric temperature and humidity data an increase in the SST of about 3°K from 8° to 14°N. However, with the present correction scheme the estimated SST does not increase toward the north; instead, it shows a small decrease of about 1° in agreement with the seasonal pattern [*U.S. Naval Oceanographic Office*, 1967] for that oceanic region.

The Nimbus 3 Iris had a ~150-km field of view, a 5-cm^{-1} spectral resolution, and a noise equivalent radiance of about 1 erg cm^{-1} sr^{-1} s^{-1} [*Hanel and Conrath*, 1969]. Although these data are slightly inferior to the Nimbus 4 Iris measurements, they can serve as a good check on the validity of the method and the magnitude of the coefficients $K(\nu)$ because we can objectively select cloud-free data in the following fashion. Measurements from the Nimbus 3 satellite of a scanning medium-resolution infrared radiometer (MRIR) with a field of view of about 50 km at nadir included the reflected solar radiation in the visible region and the infrared radiation in the 11-μm region [*Sabatini*, 1969]. Clouds can reflect solar radiation in significant amounts, whereas the ocean surface cannot. Thus with the help of the MRIR reflected solar radiation measurements at the nadir it is possible to select cloud-free Iris data objectively. During a period of 10 days in April 1969 a sample of 106 Iris measurements over the oceans was extracted when corresponding ship measurements of the SST's were available within ±1° of latitude and longitude. These data covered the globe from 60°S to 60°N. The SST's derived from these Iris data are compared with the ship data in Figure 5. We see that over a wide dynamic temperature range of about 40°–85°F (4°–29°C) the two sets of data agree very well. The rms difference between the two sets of data is about 2.5°F (1.3°C). However, the SST measured by ships has an error of about 1°C [*Saur*, 1963], and so a part of the above rms difference may be due to the error in the ship data.

In order to examine if there is any systematic bias in the Iris SST with respect to ship measurements a linear regression analysis is performed to obtain a line of best fit (Figure 5). One can notice that this regression line does not coincide with the line of perfect agreement, which would be inclined at 45° to the axes. It appears that the use of $K(\nu)$, given in Table 4, leads to a slight underestimation of the SST over cold water in high latitudes and to an overestimation of the SST in the tropics. A further refinement in the magnitude of $K(\nu)$ eliminates this systematic bias and improves the accuracy of determining the SST to about 1°C.

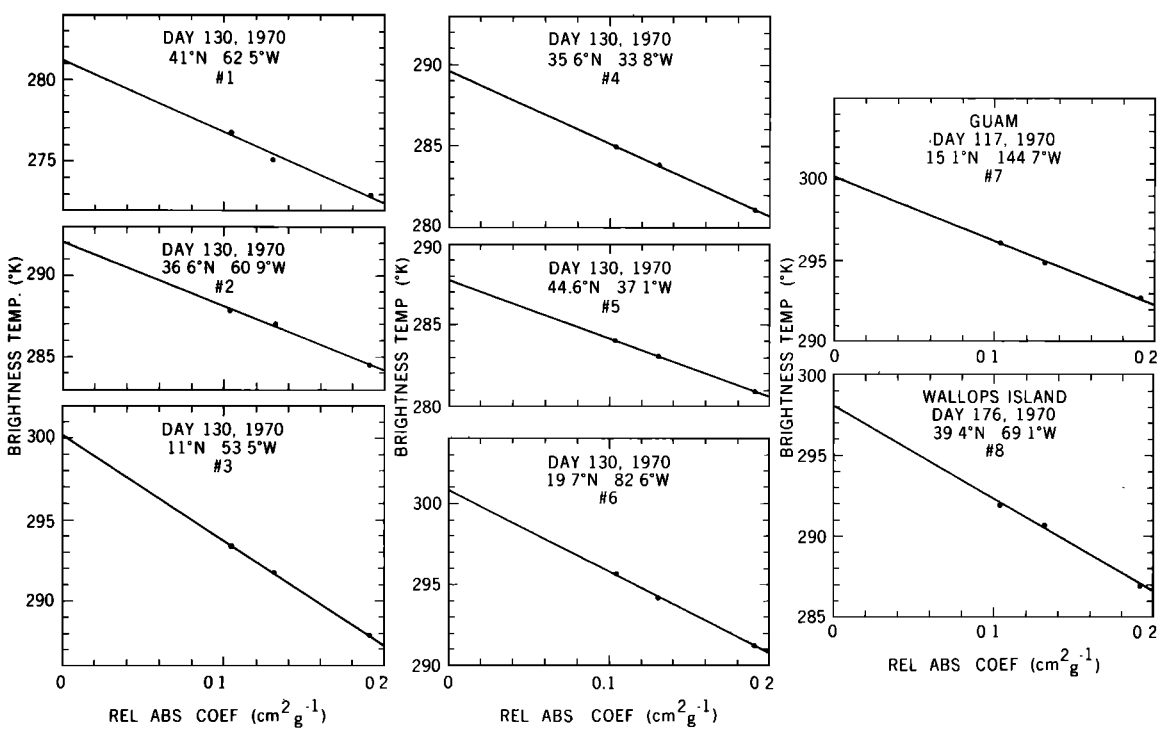

Fig. 3. Iris window brightness temperature versus relative absorption coefficient.

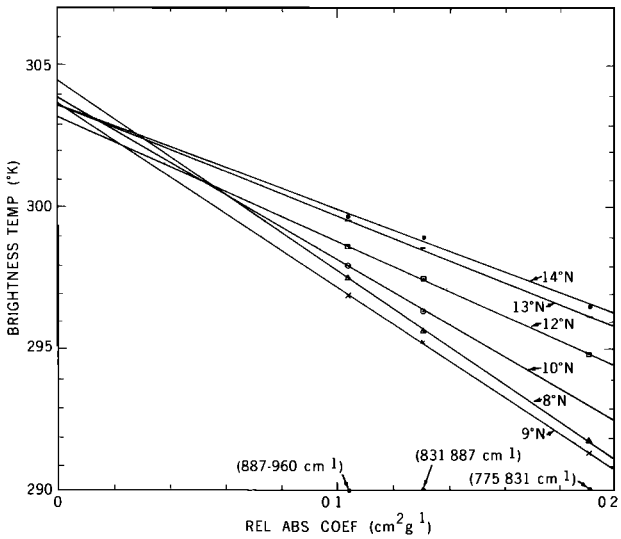

Fig. 4. Window brightness temperature variation over the Arabian Sea between 8°N and 14°N along 55°E longitude on May 10, 1970, from Nimbus 4.

Conclusion

The basic result of this study is that over cloud-free oceans we can make use of the differential water vapor absorption properties of the 11-μm window region to correct for the atmospheric attenuation. This correction scheme inherently takes into account the temperature and humidity structure prevailing at the location. Although three measurements in the window region 775–960 cm^{-1} were used to demonstrate this method, in principle, two measurements are sufficient. The two window measurements may preferably be in the approximate regions 775–831 and 887–960 cm^{-1} to obtain the maximum effect of differential absorption.

The spatial and temporal changes of SST in the tropics are generally small (about 2°C). The water vapor absorption correction over the tropics could range from about 4° to 8°C. Hence the technique of estimating the SST proposed in this study would be particularly valuable over the tropical oceans.

As the radiometric errors are amplified in the derived results, it will be desirable to have a radiometer capable of measuring brightness temperature accurate to 0.1°K in order to estimate the SST with an accuracy of about 0.5°K.

The scheme presented here can be adopted to any existing SST measurement program based on one window channel by adding one more channel in the window.

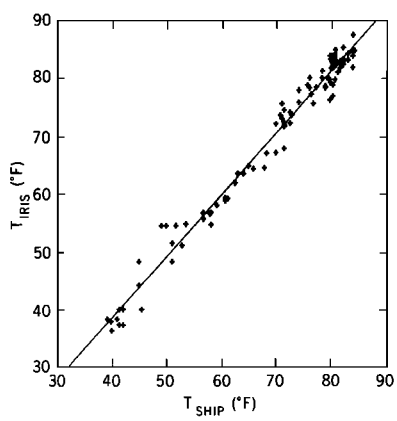

Fig. 5. Comparison of SST derived from Nimbus 3 Iris versus ship measurements.

Acknowledgments. The authors are thankful to A. Arking and B. J. Conrath for many useful discussions and to R. A. Neff of the U.S. Air Force Environmental Technical Applications Center for help in obtaining the ship measurements.

References

Allison, L. J., and J. Kennedy, An evaluation of sea surface temperature as measured by the Nimbus 1 high resolution infrared radiometer, *NASA Tech. Note, D-4078,* 25, 1967.

Anding, D., and R. Kauth, Estimation of sea surface temperature from space, *Remote Sensing Environ., 1*(4), 217, 1970.

Benedict, W. S., and L. D. Kaplan, Calculation of line widths in H_2O-N_2 collisions, *J. Chem. Phys., 30*(2), 388, 1959.

Bignell, K. J., The water vapour infra-red continuum, *Quart. J. Roy. Meteorol. Soc., 96,* 390, 1970.

Burch, D. E., Investigation of the absorption of infrared radiation by atmospheric gases, *Publ. U-4784,* p. 27, Philco-Ford Corp., Aeronutronic Div., Newport Beach, Calif., 1970.

Godson, W. L., Spectral models and the properties of transmission functions, *Proc. Toronto Meteorol. Conf., 1953,* 35, 1954.

Goody, R. M., *Atmospheric Radiation,* vol. 1, *Theoretical Basis,* pp. 128–198, Clarendon, Oxford, 1964.

Grassl, H., Separation of atmospheric absorbers in the 8–13 micrometer region, *Beitr. Phys. Atmos., 46,* 75, 1973.

Hanel, R. A., and B. J. Conrath, Interferometer experiment on Nimbus 3: Preliminary results, *Science, 165,* 1258, 1969.

Hanel, R. A., B. J. Conrath, V. G. Kunde, C. Prabhakara, I. Revah, V. V. Salomonson, and G. Wolford, The Nimbus 4 infrared spectroscopy experiment, *J. Geophys. Res., 77,* 2629, 1972.

Houghton, J. T., and A. C. Lee, Atmospheric transmission in the 10–12 μm window, *Nature Phys. Sci., 238,* 117,1972.

Kunde, V. G., and W. C. Maguire, Direct integration transmittance model, *J. Quant. Spectrosc. Radiat. Transfer, 14,* 803, 1974.

Kunde, V. G., B. J. Conrath, R. A. Hanel, W. C. Maguire, C. Prabhakara, and V. V. Salomonson, The Nimbus 4 infrared spectroscopy experiment, 2, Comparison of observed and theoretical radiances from 425–1450 cm^{-1}, *J. Geophys. Res., 79,* 777, 1974.

Lee, A. C. L., A study of the continuum absorption within the 8–13 μm atmospheric window, *Quart. J. Roy Meteorol. Soc., 99,* 490, 1973.

Platt, C. M. R., Airborne infrared radiance measurements (10- to 12-μm wavelength) of tropical east coast Australia, *J. Geophys. Res., 77,* 1597, 1972.

Prabhakara, C., B. S. Conrath, and V. G. Kunde, Estimation of sea surface temperature from remote measurements in the 11–13 μm window region, *NASA Rep. X-651-72-358,* 15 pp., 1972.

Price, J. C., Analysis of some methods for obtaining sea surface temperature from satellite observations, *NASA Rep. X-651-73-108,* 20 pp., 1973.

Rao, P. K., W. L. Smith, and R. Koffer, Global sea-surface temperature distribution determined from an environmental satellite, *Mon. Weather Rev., 100*(1), 10, 1972.

Sabatini, R. R., The Nimbus 3 user's guide, Nimbus Proj. Office, Goddard Space Flight Center, Greenbelt, Md., 1969.

Sabatini, R. R., The Nimbus 4 user's guide, Nimbus Proj. Office, Goddard Space Flight Center, Greenbelt, Md., March 1970.

Saur, J. F. T., A study of the quality of sea water temperatures reported in logs of ships weather observations, *J. Appl. Meteorol., 2,* 417, 1963.

Shenk, W. E., and V. V. Salomonson, A multispectral technique to determine sea surface temperature using Nimbus 2 data, *J. Phys. Oceanogr., 2*(2), 157, 1972.

Smith, W. L., P. K. Rao, R. Koffler, and W. R. Curtis, The determination of sea surface temperature from satellite high resolution infrared window radiation measurements, *Mon. Weather Rev., 98*(8), 604, 1970.

Stowe, L. L., The effects of particulate matter on the radiance of terrestrial infrared radiation, research report, 109 pp., Inst. of Geophys. and Planet. Phys., Univ. of Calif., Los Angeles, 1971.

U.S. Naval Oceanographic Office, Monthly charts of mean, minimum, and maximum sea surface temperature of the Indian Ocean, *Rep. SP-99,* 48 pp., Washington, D. C., 1967.

Wark, D. Q., Atmospheric transmittance used in indirect soundings of the earth's atmosphere, paper presented at International Radiation Symposium, Int. Ass. of Atmos. Phys., World Meteorol. Org., Int. Counc. of Sci. Unions, Amer. Meteorol. Soc., and Meteorol. Soc. of Jap., Sendai, Japan, May 26 to June 2, 1972.

(Received May 24, 1974;
revised July 30, 1974.)